Process Optimisation in Pulsed Laser Micromachining with Applications in Medical Device Manufacturing

K. Chen and Y. L. Yao

Department of Mechanical Engineering, Columbia University, New York, USA

Pulsed laser machining offers many unique capabilities that continuous-wave (CW) laser machining cannot. In pulsed laser machining, however, the additional process parameters of peak power, pulse frequency and pulse duration make it more difficult to find and fine tune a suitable operation window. This becomes harder in micromachining applications where tolerance of inaccuracy is smaller. How to determine these parameters in a systematic way is of great interest. This paper presents a hybrid approach, in which an analysis of the interactive relations between various process parameters and their influence on machining quality if first conducted. Based on an energy balance as well as on the characteristics of pulsed laser machining, these relationships lead to the establishment of several guidelines. These guidelines are followed to determine an initial set of process parameters that are refined in the subsequent design of an experiment. The approach is followed in a precision medical device manufacturing case where a six-variable fractional factorial design with multiple responses is chosen to quantify the effects of key process parameters on visual and metallurgical responses.

Keywords: Design of experiment; Nd:YAG laser

1. Introduction

Recent improvements in the beam quality and output power of Nd:YAG and other laser which predominately operate in pulsed modes have made them more attractive as industrial tools. Pulsed lasers produce a smaller heat affected zone and a smaller recast layer in machining applications by causing more material vaporisation through high peak power and shorter interaction time. The vaporisation usually occurs in such a short time that instead of forming a molten front as in CW machining, the on–off nature of pulsed laser machining makes the front more like a series of overlapping drilling or ablation operations. Pulsed Nd:YAG laser and especially Q-switched and frequency-doubled or quadrupled ones have found wide use in micromachining applications. The medical devices industry employs laser micromachining as a visible and sometimes as the only means to produce precision components.

Extensive trial-and-error is currently required to choose and tune the process parameters in industrial practice. The additional parameters of peak power, pulse frequency and pulse duration in pulsed laser machining greatly increase the complexity of the choice. The relations of various parameters and their effects on machining quality are not fully understood. Only limited modelling results of pulsed laser machining are available. Pulsed laser fusion cutting of stainless steel was experimentally investigated by [1], in which the beam expansion and focus position were found to influence the cut quality. Van Dijk [2] presented an experimentally based approach to optimise the pulse power, pulse length and pulse frequency by choosing the maximum cutting speed as a criterion. The metallurgical implication of lasr cutting of stainless steels was investigated by Powell and Menzies [3]. They found that when oxygen is used as the assist gas, the resolidified material is partially depleted of chromium. The change in chemistry may comprise the surface integrity that is often crucial in some medical applications such as implanting. Modelling of laser cutting has been addressed by a number of investigators. Most analytical models apply an energy balance with conduction losses derived from the classical solution of a moving heat source [4] without consideration of cut geometry. More detailed and accurate predictions require numerical models. Modest [5] developed a numerical model to predict CW or pulsed laser cutting based on a 3D conduction model. The oxidation and gas jet effects in laser cutting were addressed numerically [6,7]. These models, however, are often assumption-laden or computationally intensive, and therefore become impractical for industrial applications. An effective approach to optimise the process parameters is thus of much interest.

In this paper, a hybrid approach is developed to optimise the process parameters for pulsed laser cutting. Starting with an analysis of the mechanisms involved in pulsed laser cutting, several guidelines are proposed in conjunction with a simple energy balancing to determine the initial values of essential porcess parameters. These values are further refined in a

Correspondence and offprint requests to: Dr Y. L. Yao, Department of Mechanical Engineering, Columbia University, 220 S. W. Mudd, Mail Code 4703, 500 West 120th Street, New York, NY 10027, USA. E-mail: yly1@columbia.edu

subsequent design of experiment (DOE) exercise. The approach is implemented in laser machining of precision micro-implants in medical device industry.

2.   Analysis and Guidelines

During laser cutting, a dynamic equilibrium exists in the cut zone that balances the "incoming" energy with the "outgoing" energy. The "incoming" energy includes the absorbed laser power by the workpiece, the exothermic reaction energy, and the gas kinetic energy; the "outgoing" energy includes the energy used for cutting (heating up and phase change of the material), and the energy loss by transmission, conduction, convection and radiation. The balance is largely determined by three important parameters: laser power, cutting speed, and gas pressure. Larger reductions in laser power or increases in cutting speed will result in incomplete penetration of the cut zone, or poor cut quality. On the other hand, overheating can lead to burning. In pulsed laser cutting, the laser power is set by three additional parameters, i.e. peak power, pulse duration, and pulse frequency. The multiplication of these three parameters determines the average power of the laser. Because of high peak power, the workpiece material impinged upon by the laser beam is heated up to vaporisation temperature almost instantaneously. The mechanism of vaporisation involved in pulsed laser cutting can reduce the recast layer and heat affected zone. The peak power, pulse duration, and pulse frequency, together with the cutting speed and gas pressure, must follow certain relationships without which the mechanisms of pulsed laser cutting may break down. These relationships are outlined in the following subsections.

2.1   Peak Power

The peak power must be large enough to vaporise the workpiece. There exists a threshold value of laser beam intensity below which no melting/evaporation will occur. When a laser (without gas jet) heats a metal target, the energy absorbed is conducted into the surrounding colder metal. For steels, if the absorption rate is low ($<10^5$ W cm^{-2}, about 2 W for a spot size of 50 μm in diameter) compared to the rate of conduction, the target surface will remain below the melting point. At higher absorption rates, the surface region of the metal will melt and perhaps begin to vaporise. At even higher absorption rate ($>10^7$ W cm^{-2}, about 200 W for a spot size of 50 μm in diameter), vaporisation becomes the dominant mechanism of material removal from the target [8]. The calculation of vaporisation energy intensity is referred to in Appendix A. When the power density becomes too high, however, the gas near the spot where the laser interacts with the workpiece material is instantly transformed to plasma. The plasma formation has been shown to cause some form of material damage such as microcracks.

2.2   Pulse Duration

Theoretically, the pulse duration should be not shorter than the penetration time of the laser beam. The time needed to

Table 1. The relationship between overlapping number and overlapping area.

Overlapping number	1	2	3	4	5	6	7
Overlapping percentage (%)	39	68.5	78.9	84.2	87.3	89.5	90.9

elevate from ambient to vaporisation temperature can be roughly calculated by the analytical solution of heat supply over the circular spot [9] (Appendix B). For instance, it takes about 0.26 μs to elevate the surface temperature at the centre to the vaporisation temperature (about 3000 K for stainless steel) if the peak power is 200 W. More accurate calculations of penetration time can be obtained from modelling work based on temperature propagation velocity [8]. An experimental study of penetration time with a single laser pulse was carried out by Rohde and Dausinger [10]. They show that, for material thickness of 0.08 mm, the penetration time is the same for all pulse durations and gas pressures (less than 10 μs). Above 0.08 mm the penetration time grows faster with longer pulse durations. The penetration time decreases as the pulse energy (i.e. product of peak power and pulse duration) increases.

2.3   Pulse Frequency and Cutting Speed

Because of the periodic nature of the heating, the mechanism of pulsed laser cutting is different from that of CW laser cutting. The overall effect of laser cutting in pulsed mode is similar to overlapping a series of drilling operations. Every pulse peak makes a hole in the workpiece. Thus, in order to achieve a good quality cut, it is necessary for successive spots to overlap each other to some extent. The extent of overlapping can be represented by an overlapping number $n = rf/v$, where r is the spot radius, f the pulse frequency, and v the cutting speed. The relationship between the overlapping number and the overlapping area is as shown in Table 1.

The lower limit of overlapping is about 4. A suitable value of the overlapping number should lie between 4 to 6 to ensure an overlapping area of about 85%–90%. Higher frequency will increase the overlapping number and reduce the cut roughness. However, there is an upper limit of pulse frequency beyond which the pulse duration will be limited and pulsing will approach a continuous wave. The inverse of the pulse frequency, that is, the pulse period should be larger than the pulse duration.

2.4   Gas Pressure

The primary purpose of applying a gas jet is to remove the melt/vapour generated by a high-energy laser beam, and possibly to provide exothermic heat. For CW laser cutting of mild or stainless steel, since the reactive energy constitutes a large percentage of the total energy, the cutting speed and the cut quality are sensitive to the gas pressure. However, for pulsed laser cutting of steels, especially when thin sections are cut, the reactive energy is less significant, and the cutting speed and the cut quality are not sensitive to the gas pressure. On the other hand, the gas pressure must be increased when the

cutting speed increases in order to improve the removal capability. The gas pressure cannot be too high because the violent behaviour of turbulence will influence the cut quality. When the peak power is high enough such that almost all the material is vaporised, the gas pressure is not an important issue since the vapour is much easier to remove than the melt.

The above relationships are shown in Fig. 1. Although the relationships are complicated, a feasible yet reliable solution for process optimisation is developed and explained in the following section. The solution consists of two steps:

1. Calculation of the initial values of key process parameters based on the above analysis and understanding of the relationships.
2. Experiments to refine the process parameters.

3.   Optimisation Approach

3.1   Calculation

Based on the analysis in Section 2, the process parameters of cutting speed (v), average power (P_{ave}), peak power (P_p), pulse duration (λ) and pulse frequency (f) are related by the following equations:

1. *Energy balance equation*

$$\alpha P_{ave} = f\pi r^2 d\rho(c_p\Delta T + L_l + m'L_v)$$
$$+ 2\pi dKT \exp(-vr/2\kappa)/K_0(vr/2\kappa) \tag{1}$$

where α is the absorption coefficient, r the radius of beam spot, d the material thickness, ρ the material density, c_p the heat capacity, and ΔT the relative elevated temperature. L_l and L_v are latent heat of fusion and vaporisation, respectively. The term m' is the fraction of material vaporised, K the heat conductivity, T the elevated temperature, κ the heat diffusivity and K_0 stands for Bessel functions of the second kind. The first term on the righthand side of Eq. (1) represents the energy used for heating and phase change. A large amount of laser

Fig. 1. The relationships of the various process parameters in pulsed laser machining.

power is transmitted owing to overlapping of consecutive pulses. The second term on the righthand side is the conduction loss, which is derived from the theory of a moving heat source [4]. Schulz et al. [11] gave a correlated analytical solution of conduction loss taking into the account of cylindrical heat source:

$$P_{con} = \rho c_p \Delta Tv2rd(Pe/2)^{-0.7}$$

where P_{con} is the conduction loss and Pe is the Péclet number, which equals rv/K. In Eq. (1), the convective and radiative loss are neglected, so is the reaction energy when a reactive gas is applied. The conduction loss during the on and off period is simply combined and represented by the analytical solution of the moving heat source. For cutting thick sections using an oxygen jet, a lumped per cent of reaction energy can be added to the left-hand side of the energy balance equation.

2. *Average power relation*

$$P_{ave} = P_p\lambda f \tag{2}$$

It should be noted that the multiplication of the peak power and pulse duration ($P_p t$) is the so-called pulse energy.

3. *Overlapping condition*

$$n = rf/v \geq 4 \tag{3}$$

4. *Low limit of peak power*

$$P_p \geq \text{Vaporisation intensity} \tag{4}$$

These relationships form the basis of a method to determine the initial values of the process parameters in pulsed Nd:YAG laser cutting of steels and the approach can be extended to other materials. The procedure for applying the method is as follows:

1. Choose an overlapping number to guarantee the cut quality ($n = 4$ to 6 suggested).
2. Choose the peak power to ensure vaporisation of the material.
3. Choose a relatively high frequency to ensure enough cutting speed but to guarantee enough peak power.
4. Determine the cutting-speed range based on the beam spot size and the overlapping number.
5. Determine the average power, based on the energy balance.
6. Determine the pulse duration, based on the pulse energy and the peak power.

Iterations may be necessary to reach balanced values of these parameters when all the relations in Fig. 1 are taken into consideration. The system limitations of peak power, pulse frequency and pulse duration must also be considered.

3.2   Experiment

The analytically determined process parameters are further verified and refined by design of experiment (DOE). The response(s) should be identified based on the nature and type of the finished products. The critical parameters are chosen based on the analysis of their effects on the response variables.
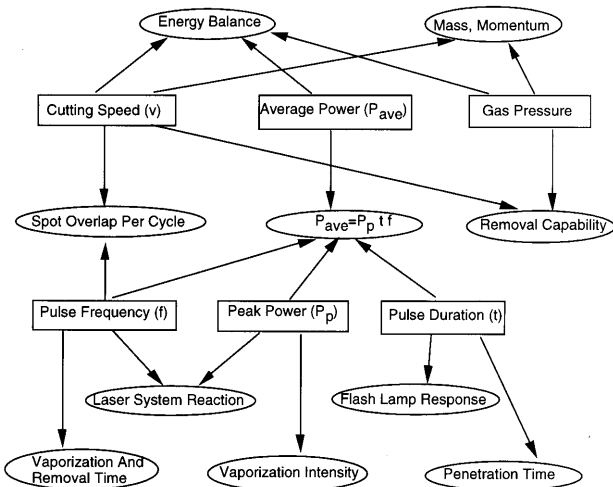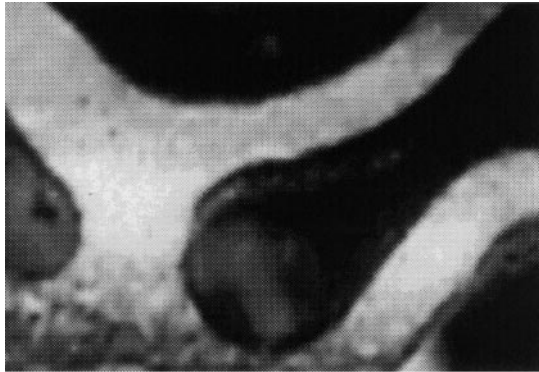
Table 2. Two-level factorial design.

Independent variable	Low	High
Pulse duration	0.1 ms	0.125 ms
Average power	2 W	3 W
Cutting speed	2.3 in min^{-1}	3.5 in min^{-1}
Orifice size	30 mil	40 mil
Gas pressure	30 p.s.i.	60 p.s.i.
Water flowrate	2 gal/h	3.5 gal/h

Fig. 2. Good surface finish (80×) (t = 0.1 ms, P_{ave} = 2 W, orifice size = 40 mil, v = 3.5 in min^{-1}, gas = 30 p.s.i., water = 2 gal/h).

These parameters may not necessarily be the same as the above parameters.

A DOE typically starts with a factorial design. A fractional factorial experiment allows the average and interactive effects of the process variables on the response(s) to be determined by a minimum number of experiments. Although the results from the factorial experiments do not point directly to the optimal points of the process variables, they form the basis for optimisation via response surface methodology where additional experiments will be specified interactively. Montgomery [12] gives more details on DOE, including response surface methodology.
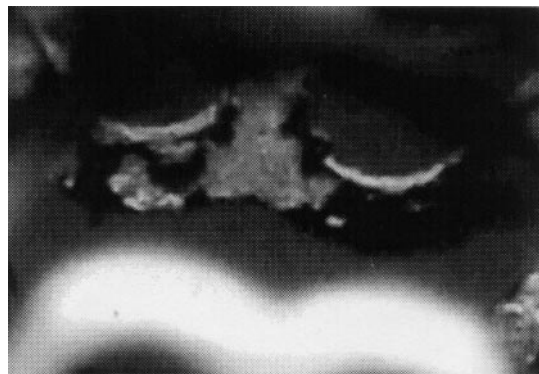
Fig. 3. Excessive dross attachment (80×) (t = 0.1 ms, P_{ave} = 3 W, orifice size = 40 mil, v = 3.5 in min^{-1}, gas = 30 p.s.i., water = 3.5 gal/h).
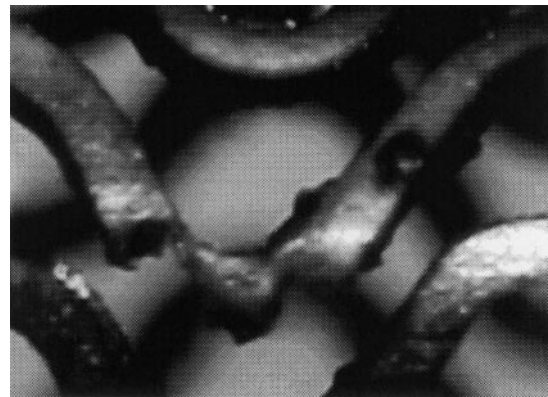
Fig. 4. Severe burns (80×) (t = 0.125 ms, P_{ave} = 3 W, orifice size = 40 mil, v = 2.3 in min^{-1}, gas = 60 p.s.i., water = 2 gal/h).

4.   Application in a Precision Medical Device Manufacturing Case

4.1   Calculation and Experimental Conditions

A stainless steel design of implant is tubular-shaped without a typical diameter of 1.5 mm and thickness of about 100 μm. Slots of about 40 μm wide are cut by pulsed Nd:YAG laser. Water is pumped through the tubing to carry away debris and to prevent possible burning on the opposite side of the tubing.

The initial values of key process parameters are calculated following the above-described steps. The laser energy intensity for vaporisation was calculated according to [9] (see Appendix B). The result is $I > 1.04 \times 10^7$ W cm^{-2} (about 118 W peak power for a spot size of 38 μm). The overlapping number is chosen as 4.5. The maximum pulse frequency of 300 Hz, for the laser system used, is considered not to be too high and is therefore chosen. Based on the overlapping number, pulse frequency and beam spot size, the cutting speed is determined to be 2.99 in min^{-1} (Eq. (3)). The average power was calculated to be 3.54–4.43 W according to Eq. (1) (see Appendix C for physical properties and constants used in the calculation). The pulse duration was found to be 0.1–0.125 ms from Eq. (2).

These initial values are refined because of the necessary assumptions and simplifications made in the calculation. Additional parameters may also need to be further considered for particular applications. Although gas pressure may be less influential in thin section cutting as mentioned earlier, it may need to be considered for this implant application because among the undesirable characteristics of implants produced by this method are the presence of microcracks and dross attachments, and a thick and non-uniform recast layer. This argument is also applicable to water flowrate. They are therefore also chosen as independent variables in a subsequent 2-level factorial design as shown in Table 2.

The average power values are reduced to account for the fact that oxygen and water are used. Oxygen typically contributes as much power as the laser does, but water flow carries away heat. Nozzle orifice size is thought to be important in influencing flow patterns that in turn affect the extent of dross attachment and the recast layer. The values of orifice size, gas pressure and water flowrate are empirically determined. The
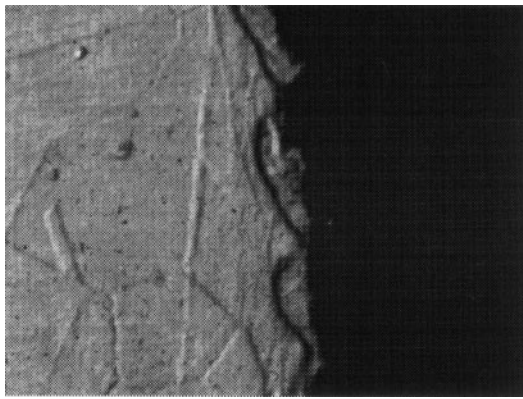
Fig. 5. Recast layer ($1000\times$) ($t = 0.125$ ms, $P_{ave} = 3$ W, orifice size $= 30$ mil, $v = 2.3$ in min^{-1}, gas $= 30$ p.s.i., water $= 2$ gal/h).

remaining factors such as beam diameter, focal length, beam mode, standoff, focus position, water temperature are kept constant.

The responses (dependent variables) of the experiments are chosen in line with the quality requirement. The cut quality of the laser is evaluated by the overall surface finish and the recast layer thickness. A minimal recast layer is desired. The recast layer consists of an oxide layer formed from the assist gas. The oxide layer has a different coefficient of expansion from the metal, resulting in crack formation. The surface finish may consist of dross attachment. Dross attachment is formed from a molten metal oxide that solidifies unevenly at the exit of the cut. Dross is also a source of cracks owing to its brittleness and it is hazardous to balloons. Another important phenomenon affecting the overall surface finish is the burn marks. Burns results from overheating and occur particularly at starting/finishing points or at corners where the cutting speed has to reduce.

A 2^{6-1} fractional factorial experiment was carried out. All 6 main effects and 15 two-variable interactions are obtainable assuming that three or more variable interactions are negligible. To keep the number of experiments and subsequent analysis

manageable, four replications of each experiment were performed. This corresponds to about a 75% confidence level and an allowable deviation from the sample average of approximately 0.5 standard deviation. Dross attachment was inspected visually using an optical comparator and rated on a scale of 1 to 5, with 1 the best and 5 the worst. Burn mark was also optically inspected and rated on a scale of 1 to 3, with 1 being no/little sign and 3 having a very visible brownish mark. Burn through, incomplete and cracks were recorded as the worst case. Recast layer thickness was measured by using microscopy after each implant after being mounted on epoxy and polished.

4.2 Experimental Results

The finish quality varies from cuts without visible burning marks and dross attachment, to cuts with excessive burns, dross attachment or cracks. Figure 2 shows part of an implant with a good surface finish. Figure 3 shows excessive dross attached to the inner side of an implant, for which excessive water flow may be responsible. A cutting speed that is too high will also cause this problem. Figure 4 shows severe burns on the cuts when there is excessive laser power or oxygen supply. Figure 5 shows a recast layer at the cutting edge. Some striation pattern beneath the recast layer can also be seen.

Standard DOE analysis was carried out in order to quantify the effects of process parameters (factors) and their interactions on dross attachment, burn and recast layer thickness (responses), to identify significant factors, and to provide a basis for subsequent optimisation. For simplicity, only the analysis results for dross attachment are presented. The half-normal plot on Fig. 6 shows that the significant factors affecting dross attachment are *B* (average power), *C* (orifice size) and *D* (cutting speed), and significant interactions are *BD* and *BC*. Their relative significances are indicated by their degree of deviation from the half-normal curve. A predicative model is resulted as:

$$\text{Dross} = 2.67 - 0.17 * B + 0.20 * C + 0.73 * D$$
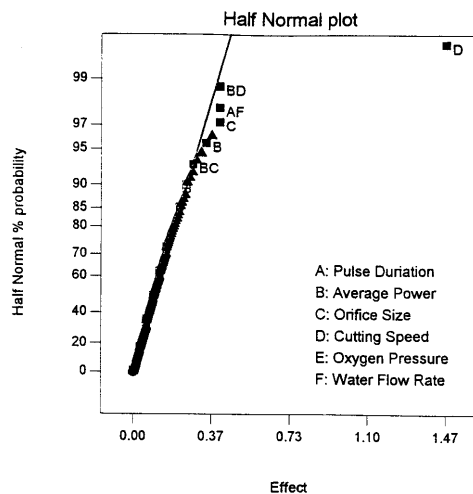$$+ 0.14 * B * C - 0.20 * B * D \qquad (5)$$
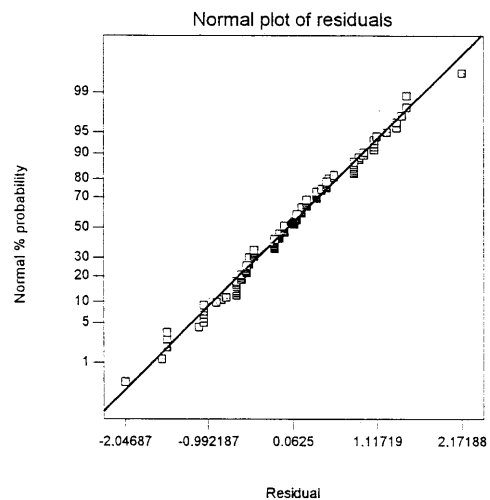

Fig. 6. Half normal plot of dross.

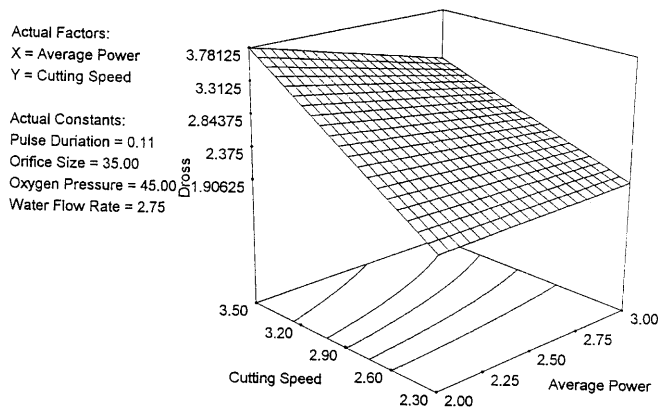**Fig. 7.** Half normal plot of residuals.

Fig. 8. Interactive effects of average power and cutting speed on dross.

This equation is in terms of coded factors. The results are consistent with a physical understanding of the process. For instance, when the average power (B) increases, the dross attachment rating number decreases, meaning less dross. Orifice size (C) is identified as a significant factor. This may well indicate that orifice size not only controls the actual pressure at its exit but also affects the flow pattern near the cutting front.

The statistical "goodness" of such a model is measured in an F-test. An F-value of 28.99 is obtained which indicates that change seen in dross is mainly caused by process parameters instead of by randomness due to measurement errors or variations between replications. The normal plot of residuals (difference between experimental measurement and prediction by the above model) on Fig. 7 confirms the model goodness.

The interactive effects can also be seen. For instance, the interactive effects of average power and cutting speed on dross are shown in Fig. 8. As seen, the effect of speed on dross is not influenced much by the power, but the opposite is not true. At higher speeds, the increase of power improves the dross attachment, while at lower speed, power seems to have little effect on dross. These trends are consistent with the physical understanding. Similar results are shown in Fig. 9 for the interactive effects of average power and orifice size on dross.
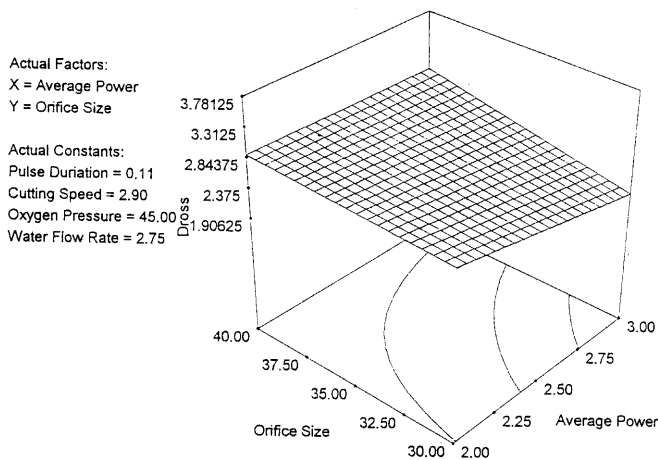

Fig. 9. Interactive effects of average power and orifice size on dross.

The predictive model is normally applicable only under operation conditions not too far away from that used to generate the model because of the underlying assumption of linearity used in DOE. The response surface methodology based on a 3-level factorial experiment could further refine the results but would require additional experiments. However, the results based on a 2-level factorial experiment have provided much useful information.

5. Summary

Extensive trial-and-error is currently required in industry to determine the process parameters involved in pulsed laser machining. Such an approach can be time-consuming and yet may not reach an optimal solution. On the other hand, most analytical or numerical methods require extensive computation and substantial simplifying assumptions and thus are impractical for industrial application. The optimisation method presented in this paper takes a hybrid approach to combine a simple analytical prediction with a DOE experiment. By following several guidelines derived from an analysis of key relationships in pulsed laser machining, the initial values of the process parameters are determined. These values are further refined by a subsequent DOE experiment. The application of the optimisation approach in a medical device manufacturing case is presented.

References

1. M. Geiger and A. Gropp, "Laser fusion cutting of stainless steel with a pulsed Nd:YAG laser", Welding in the World, 31(3), pp. 22–26, 1993.
2. M. H. H. Van Dijk, "Pulsed Nd:YAG laser cutting", Annual Review of Laser Processing, Industrial Laser Handbook, pp. 52–64, 1990.
3. J. Powell and I. A. Menzies, "Metallurgical implication of laser cutting stainless steels", Power Beam Technology, pp. 3–18, September 1986.
4. H. S. Carslaw and J. C. Jaeger, Conduction of Heat in Solids, Oxford University Press, 1959.
5. M. F. Modest, "Laser through-cutting and drilling models for ablating/decomposing materials", Journal of Laser Applications, 9, pp. 137–145, 1997.
6. K. Chen, Y. L. Yao and V. Modi, "Numerical simulations of oxidation effects in laser cutting of mild steels", ICALEO '97, 83, Sec. B, pp. 37–45, 1997.
7. K. Chen, Y. L. Yao and V. Modi, "Numerical simulation of gas jet effects in laser machining", ICALEO '98, 84, Sec. B, pp. 120–129, 1998.
8. R. S. Patel and M. Q. Brewster, "Gas-assisted laser-metal drilling: theoretical model", Journal of Thermophysics, 5(1), pp. 32–39, 1991.
9. F. W. Dabby and U. Paek, "High-intensity laser-induced vaporization and explosion of solid material", IEEE Journal of Quantum Electronics, QE-8(2), pp. 106–111, 1972.
10. H. Rohde and F. Dausinger, "The forming process of a through hole drilled with a single laser pulse", ICALEO '95, pp. 331–340, 1995.
11. W. Schulz, D. Becker, J. Franke, R. Kemmerling and G. Herziger, "Heat conduction losses in laser cutting of metals", Journal of Physics, D: Applied Physics, 26, pp. 1367–1363, 1993.
12. D. C. Montgomery, Introduction to Statistical Quality Control, 3rd edn, John Wiley, 1996.

Appendix A. Vaporisation Energy Intensity

Most modelling work gives the transient analytical solution of heat-conduction equation in one-dimension or multi-dimensions. An important parameter is the temperature propagation velocity after vaporisation temperature is reached. This depends on the impinging laser intensity and the mechanical properties of the material. If the velocity is negative, this means that the incident laser intensity is insufficient to maintain the front surface at the vaporisation tempera-ture. According to Dabby and Paek [9], the positive velocity will produce the following relationship:

$$\alpha I > Kc^2 T_v \tag{A1}$$

where I is the energy intensity, α the absorptivity, K the heat conduc-tivity and T_v is the vaporising temperature. The term c is a constant, which is used to be a fitting parameter that would most closely match the determined initial temperature profile, based on:

$$T = T_v(1 + cz)e^{-cz}, \tag{A2}$$

where z is the distance from the surface in the penetration direction. The laser energy intensity for vaporisation this can be evaluated.

Appendix B. Penetration Time

The penetration time is very complicated to calculate because of the phase transition involved. According to Dabby and Paek [9], the dimensionless propagation velocity will be

$$u = 1 - \exp(B^2\tau) \, erfc \, (B \sqrt{\tau}) + 2\lambda C^3 \, \tau \exp(C^2\tau) \, erfc(C \sqrt{\tau}) - \frac{2\lambda}{\sqrt{\pi}} C^2 \sqrt{\tau} \tag{A3}$$

where the dimensionless parameters are defined as

$$\tau = (I^2 c_p/\rho K L_v^2)t \qquad u = (\rho L_v/I)U$$
$$\lambda = c_p T_v/L_v \qquad B = (K\alpha L_v)/(Ic_p)$$
$$C = (KcL_v)/(Ic_p)$$

The symbols used are defined in the Nomenclature section. The penetration time can be calculated based on

$$\int_0^t u\mathrm{d}t = d, \tag{A4}$$

where d is the material thickness.

Appendix C. Physical Properties and Constants for Calculation

See Table A1.

Table A1. Physical properties and constants for calculation.

Kerf width: 0.038 mm	Workpiece thickness 0.089, 0.178 mm
Heat capacity 500 J $(\text{kgK})^{-1}$	Heat conductivity 14.9 W $(\text{mK})^{-1}$
Latent heat of fusion 300 kJ kg^{-1}	Latent heat of vaporization 6500 kJ kg^{-1}
Steel density 7900 kg m^{-3}	Heat diffusivity 3.8×10^{-6} m^2 s^{-1}
Ambient temperature 300 K	Vaporisation temperature 2800 K

Nomenclature

c	constant
c_p	heat capacity
d	workpiece thickness
f	pulse frequency
I	laser intensity
K	heat conductivity
K_0	Bessel function of second kind
L_l	latent heat of fusion
L_v	latent heat of vaporisation
m'	fraction of material vaporised
n	overlapping number
P	laser power
P_{ave}	average power
P_{con}	conduction loss
Pe	Péclet number
P_p	peak power
r	laser beam spot radius
t	time
T_v	vaporising temperature
u	temperature propagation velocity
v	cutting speed
z	distance into workpiece
λ	pulse duration
ΔT	relative elevated temperature
α	absorptivity
κ	heat diffusivity (m^2 s^{-1})
ρ	material density